



Kinetic study of soybean oil methanolysis using cement kiln dust as a heterogeneous catalyst for biodiesel production

E.G. Al-Sakkari^{a,*}, S.T. El-Sheltawy^a, N.K. Attia^b, S.R. Mostafa^a

^a Department of Chemical Engineering, Faculty of Engineering, Cairo University, Egypt

^b National Research Center, Dokki, Egypt

ARTICLE INFO

Article history:

Received 28 September 2016

Received in revised form 6 December 2016

Accepted 3 January 2017

Available online 16 January 2017

Keywords:

Cement kiln dust

Biodiesel

Transesterification kinetics

Heterogeneous catalysis

ABSTRACT

Biodiesel may be produced through transesterification reaction between triglycerides and light alcohols in presence of different catalysts. This paper presents a study of kinetics of soybean methanolysis using cement kiln dust (CKD) as a heterogeneous catalyst. All reactions took place at a constant methanol to oil molar ratio of 12:1 and catalyst loading of 3.5%. The study consists of three phases; the first one is to consider the reaction following irreversible homogeneous kinetic models (1st and 2nd orders) due to using high excess of methanol. The second is to add the backward reaction term to the power law models. Finally, models for heterogeneous catalysts such as Eley–Rideal and Langmuir–Hinshelwood models are suggested to describe reaction kinetics. Least squares method, Runge–Kutta methods for ordinary differential equations and Levenberg–Marquardt algorithm for minimizing objective function were used to obtain the parameters of each suggested model in each phase. Calculation of determination coefficient (R^2) and minimization of squared error summation method were used to determine which model is the best one to fit the experimental data. Eley–Rideal kinetic model was the best model amongst the suggested models. Fisher and Chi-square criteria were used to check the reliability of generated rate equation. The rate differential equation was solved to obtain the main engineering factors controlling the reaction.

© 2017 Elsevier B.V. All rights reserved.

1. Introduction

Biodiesel is a mixture of monoalkyl esters produced through transesterification reaction between triglycerides and light alcohols such as methanol and ethanol. Triglycerides sources can be virgin or used edible oils [1] or non edible oils [2,3].

Typical edible oils which are widely used for biodiesel production are soybean and sunflower oils; also, these oils can be utilized as feedstocks after being used in cooking or frying [4]. Recently, there is a general interest amongst research studies to produce biodiesel from non edible sources [5,6]. Some of the famous non-edible oils used are karanja oil [7], pongamia oil [8,9] jatropha oil [9] and oils extracted from microalgae [10]. These studies aim to optimize different reaction parameters as well [11,7]. They are concerned about the optimization of these conditions in the sake of the development of biodiesel mass production. Factorial design and response surface methodology concepts are widely used

techniques for studying different factors affecting transesterification as well as their optimization [12,8].

Kinetics of transesterification reactions are well studied by many researchers [13–15]. These studies are concerned in generating expressions for reaction rate to help designing a proper reactor to produce biodiesel from triglycerides. Reaction rates take different forms according to the catalyst used [16]. In the case of homogeneous catalyzed transesterification the reaction rate can take the form of power law rates (i.e. first or second order) [17]. On the other hand, in the case of using heterogeneous catalysts, reaction rate takes other forms [18]. These formulas are elaborated taking into consideration the different mechanisms of reaction and the controlling step of this reaction [19]. In the case of using solid catalyst, controlling step can be the reaction step adsorption of reactants, desorption of products or a mass transfer step [20]. Mass transfer steps include the external and internal diffusion relative to the catalyst pellet [21].

There are two famous mechanisms which are: Eley–Rideal mechanism and Langmuir–Hinshelwood mechanism. The former mechanism involves the reaction of an adsorbed molecule on a certain site with another molecule in fluid phase to produce two products one of them is adsorbed while the other one is free in

* Corresponding author.

E-mail address: egomaa123@yahoo.com (E.G. Al-Sakkari).

Nomenclature

Abbreviations

%x	Percentage conversion
TG	Triglyceride (soybean oil)
MA	Methanol
DG	Diglyceride
MG	Monoglyceride
FAME	Fatty acid methyl ester (biodiesel)
CA	Concentration of component a (mol L^{-1})
DAB	Diffusivity of a in B
Deff	Effective diffusivity
GL	Glycerol
r	Rate ($\text{mol L}^{-1} \text{ h}^{-1}$)
t	Time (h)
(k ₁)	Rate constant of forward reaction of TG → DG
(k ₂)	Rate constant of backward reaction of TG → DG
(k ₃)	Rate constant of forward reaction of DG → MG
(k ₄)	Rate constant of backward reaction of DG → MG
(k ₅)	Rate constant of forward reaction of MG → G
(k ₆)	Rate constant of backward reaction of MG → G
(k _f)	Rate constant of forward reaction of TG → G (overall reaction)
(k _b)	Rate constant of backward reaction of TG → G (overall reaction)
K	Rate constant includes the constant methanol concentration
(k _{ad})	Rate constant of forward reaction of adsorption of methanol
(k _{ad-})	Rate constant of backward reaction of adsorption of methanol (ER)
(k _s)	Rate constant of forward reaction of surface reaction (ER)
(k _{s-})	Rate constant of backward reaction of surface reaction (ER)
(k _d)	Rate constant of forward reaction of desorption of glycerol (ER)
(k _{d-})	Rate constant of backward reaction of desorption of glycerol (ER)
S	Active site
Sp	Particle surface area
(K _{d'})	Equilibrium constant of reaction of adsorption of methanol (ER)
(K _{d''})	Equilibrium constant of reaction of desorption of glycerol (ER)
C _t	Concentration of total active sites
C _v	Concentration of empty active sites
K', K'' and K _i ' Constants	
k _m	Mass transfer coefficient
E	Activation energy
A ₀	Pre-exponential factor
R	Universal gas constant
V _p	Particle volume
η	Effectiveness factor
ε	Porosity
τ	Tortuosity
ρ	Density
μ	Viscosity
ϕ	Thiele modulus
d _p	Particle diameter
ω	Angular velocity
UL	Linear velocity

D _r	Reactor diameter
Sh	Sherwood number
Re	Reynolds number
Sch	Schmidt number

the fluid phase [22]. On the other hand, Langmuir–Hinshelwood mechanism involves single site mechanism or dual-site mechanism surface reaction [23].

Noureddini and Zhu [24], Bambase et al. [25], Karmee et al. [26] and Vicente et al. [27] suggested a second-order reaction mechanism during the transesterification of soybean oil using homogeneous catalyst. Darnoko and Cheryan [28] reported that the reaction mechanism would be of second-order in the early stages of reaction shifting to first order mechanism in latter stages.

All previously cited works assumed that the reaction is kinetically controlled and that the side reactions – saponification and neutralization of free fatty acids- are negligible [29]. However, Bambase et al. [25], Darnoko and Cheryan [28] and Noureddini and Zhu [24] selected the step of triglyceride conversion to diglyceride as controlling step while Karmee et al. [26] suggested the conversion of diglyceride to monoglyceride as determining step and Vicente et al. [27] selected conversion of monoglycerides to glycerol reaction as being the controlling step.

Dossin et al. [30] and Hattori et al. [31] reported methanol adsorption step as the main controlling step using heterogeneous catalyst, while Xiao et al. [32], Dossin et al. [30] and Hattori et al. [31] suggested surface reactions step. Eley–Rideal (ER) and Langmuir–Hinshelwood–Hougen–Watson (LHHW) mechanisms are the proposed mechanisms for heterogeneously catalyzed transesterification. On using a solid catalyst that contains Lewis acid/base sites the reaction can be described by LHHW model [32]. Dossin et al. [30] and Hattori et al. [31] claimed that ER kinetic model was suitable for heterogeneous base catalysts. Both LHHW and ER models are not suitable for describing reactions catalyzed by a heterogeneous catalyst leaches into the reaction mixture as this catalyst cannot be considered totally heterogeneous, so these reactions can follow the models proposed for homogeneous reactions (i.e. first and second order kinetic models) [29,33].

MacLeod [34] fitted power law, ER and LHHW models with the experimental data obtained by using alkali metals doped on metal oxides (e.g. Li–CaO) as solid catalysts. Due to catalyst leaching, homogeneous contribution was found to be significant so the second order model was used to describe the reaction kinetics as an initial solution. On comparing the fitted data with experimental data there results are not compatible so this model was not representative. It was found that ER was the best model to represent the reaction kinetics as it had lower sum of squares error than LHHW model. However, even the ER model cannot be considered to be totally appropriate due to leaching which make the reaction partially homogeneous.

Recently the kinetics of methanolysis reaction over complex heterogeneous catalysts, prepared through simple synthesis process or derived from sustainable sources, was investigated [35]. When K₂O/NaX was used for catalyzing the methanolysis of safflower oil, it was found that the best kinetic model to fit the experimental data is a model based on Eley–Rideal mechanism while the rate determining step was assumed to be the methanol adsorption step [36]. In 2013, Kumar and Ali [37] investigated the transesterification of Low-quality triglycerides over a Zn/CaO and they observed that the reaction follows a pseudo first order kinetic model. Feyzi and Khajavia [38] studied the kinetics of biodiesel synthesis from sunflower oil using Ba–Sr/ZSM-5 nano-catalyst where they found out that the reaction can be described by pseudo

second order kinetic model. Nambo et al. [39] conducted a kinetic study on olive oil methanolysis using ZnO nano-rods synthesized via a wet chemistry approach as catalysts where it was observed that at short reaction time the reaction was controlled by mass transfer, on the other hand, as the reaction proceeded to moderate and longer time, the reaction kinetics dominated where it can be described by a pseudo first order kinetic model. The application of CaO/SiO₂, prepared through sol-gel technique, as a catalyst for biodiesel production was investigated as well as the kinetics of the reaction which obeys a pseudo first order kinetic model [40]. Kaur and Ali conducted several studies to investigate the usability of different solid catalysts to catalyze biodiesel production from different feedstocks as well as studying the reaction kinetics for these different systems [41–44]. These studies included ethanolysis of jatropha oil using molybdenum impregnated calcium oxide as solid catalyst [41], ethanolysis of waste cottonseed oil using Li/NiO heterogeneous catalyst [42], preparation and utilization of Ce/ZrO₂–TiO₂/SO₄²⁻ as solid catalyst for the esterification of fatty acids [43] and using lithium zirconate for simultaneous esterification and transesterification of low quality triglycerides [44]. It was found that the reaction in these different cases follows pseudo first order kinetics and on applying Koros–Nowak test on these systems it was demonstrated that reaction rates are independent from diffusion limitations. In addition, the kinetics of jojoba oil butanolysis over CaO derived from mussel shell was studied where it was found that the reaction can be modeled using Eley–Rideal model based on a three-step mechanism, whereas, the overall reaction was controlled by the surface reaction step [45]. On using waste mussel shells and demineralized (DM) water treatment precipitates as CaO and MgO sources in order to catalyze waste cooking oil transesterification, Moradi et al. [46] indicated that a pseudo first order kinetic model was satisfactory for modeling the reaction kinetics. Aside from these studies, Avhad et al. [47] examined the application of glycerol-enriched CaO derived from *Mytilus Gallo-provincialis* shells for catalyzing ethanolysis of avocado oil where they investigated that the reaction can obey a previously developed mathematical model [45] based on Eley–Rideal three-step mechanism however in this study of avocado oil ethanolysis the overall process was controlled by the ethanol-adsorption step.

Natural wastes can however be used as non hazardous sources of calcium such as, fertilizers, animal feed supplements and nutrients [48–50]. Other industrial wastes such as wastes from steel industries [51], waste concrete [52], wood ash [53] and cement kiln dust, can be used as sources of solid catalysts for biodiesel production. Cement kiln dust can be considered a promising source because of its high yearly production rate as well as it contains active metal oxides that have the ability of catalyzing triglycerides alcoholysis to produce biodiesel. The reuse of different industrial wastes, especially solid wastes, in other applications can be considered the recent general trend in order of reducing environmental pollution [54]. Taking into consideration material conservation as well as minimization of undesired environmental impacts, CKD was used, in many studies, as a construction material, adsorbent and fertilizer [55,56]. On the same line, using CKD can add economical value to production process as using a certain waste is a good way for process cost minimization; as in this case the price of catalyst can be eliminated or highly decreased relative to the price of other catalysts such as homogeneous KOH catalyst. CKD consists mainly of calcium oxide ranging from 19.45% to 64% by mass in addition to magnesium oxide. From literature, it may be observed that its specific surface area ranges from 0.23 m²/g to 1.4 m²/g [57], and sometimes it may reach higher values (e.g. 11.76 m²/g) [58].

The aim of this work is to study the kinetics of soybean oil methanolysis using cement kiln dust (CKD) as a heterogeneous catalyst as well as to obtain the best rate equation that fits experimental data to generate an equation which relates concentration

Table 1
Physical Properties of Soybean Oil used [59,60].

Property	Value (unit)
Density 20 °C	0.9261 g/mL
Viscosity 20 °C	58.5–62.2 cP
Specific Heat Capacity 20 °C	0.448 cal/g °C
Heat of combustion	9450–9388 cal/g
Smoke point	245 °C
Flash Point	324 °C
Fire Point	360 °C
Melting Point	0.6 °C
Pour Point	–12 to –16 °C
Cloud Point	–9 °C

with time, taking into consideration the economical issues of using such catalyst on choosing the methanol to oil molar ratio and catalyst loading (i.e. minimization of process cost by decreasing the usage of methanol and increasing the utilization of waste CKD). Finally, it will be proved that the reaction is independent from diffusion limitations through calculation of the external and internal mass transfer resistances in order to prove that they are negligible.

2. Materials and methods

2.1. Materials

2.1.1. Soybean oil

The oil used in this study is soybean oil obtained from Egyptian food market and it has the properties tabulated in Tables 1 and 2. Virgin oil was used in this study as a first step to study the feasibility of using CKD to catalyze biodiesel production to ensure that there are no contaminants in the oil during the first study. Further work will be performed using waste vegetable oil to decrease the dependence on virgin oils in biodiesel production.

2.1.2. Cement kiln dust

The catalyst used in this study was cement kiln dust (CKD) obtained from Turah Cement Factory located in Southern Cairo.

2.1.3. Methanol

Methanol (analytical grade) was used to transesterify soybean oil. It was purchased from El-Nasr Pharmaceutical Chemicals Co. (ADWIC) (Mwt. 32 and purity of 99.8%).

2.2. Methods

2.2.1. Catalyst preparation

CKD used to catalyze the reaction of soybean oil with methanol to produce biodiesel was calcined for 4 h at 740 °C to ensure that no humidity is left in the catalyst and to convert calcium carbonate into calcium oxide, the effective substance that catalyzes the transesterification reaction.

2.2.2. Catalyst characterization

Properties of used calcined CKD (CCKD) such as specific surface area, particle size distribution and chemical composition were determined. Typical chemical composition of CKD was determined using Axios XRF (Axios, Sequential WD-XRF Spectrometer, PANalytical 2005). Sieve analysis test was carried out using 90, 75, 63 and 50 µm sieves. The morphology of used CCKD was determined using

Table 2
Chemical Properties of Soybean Oil used.

Fatty Acid	Palmitic	Stearic	Oleic	Linoleic	Linolenic
Carbon Number	16:0	18:0	18:1	18:2	18:3
Percentage%	11.4	4.2	26.1	50.3	7.9

scanning electron microscope “FEI QUANTA, Inspect S microscope” while XRD analysis of this CCKD was obtained using Bruker D8 Advance XRD Analyzer. Specific surface area and the full isotherm of CCKD were obtained by applying BET gas sorption technique with nitrogen as adsorbate at 77.35 K using “Quantachrome NOVA Automated Gas Sorption System”. Average pore size and total pore volume values were determined according to DFT method using the same gas sorption system. The basic strength (H_{c}) of CCKD was determined using Hammett indicators method [52]. Thermal gravimetric analysis of used CKD was done using SDT Q600 Thermal Analysis Instrument.

2.2.3. Transesterification reaction

Transesterification was carried out in 250 ml reaction flasks heated on a hot plate and equipped with water condenser, magnetic stirrer and thermometer. Fifty grams of the oil was introduced into the reaction flask and then heated to the desired temperature. Calcined CKD was added to the oil with alcohol and the mixture was continuously stirred at 800 rpm. The mixture was filtered using Whatman ashless filter paper grade 42 (2.5 μm) to remove any suspended solids and then carefully transferred to a separating funnel and allowed to stand overnight. The lower layer (glycerol and methanol) and the upper layer (methyl esters and some methanol) were separated in two separate beakers and methanol evaporated at 105 °C. Overnight gravity separation was necessary for separating ester and glycerol layers due to their density differences. This is facilitated by the fact that the solubility of glycerol in ester-methanol layer is negligible at ambient conditions. The purity and fatty acids methyl ester composition of the produced biodiesel were characterized using Agilent HP 6890 GC system equipped with flame ionization detector (FID). The column used was hp 5 column type of 30 m length and 0.5 mm internal diameter. Percentage conversion was estimated using glycerol base by weighing the produced glycerol [61,62]. At complete conversion, one mole of oil produces one mole of glycerol. On mass basis, 50 g of oil produce about 5 g of glycerol.

$$\% x = \frac{\text{weight of produced glycerol}}{\text{weight of produced glycerol at complete conversion}} * 100\% \quad (1)$$

For 50 g of oil, the conversion can be calculated by Eqn.2:

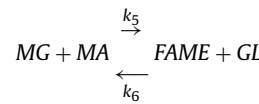
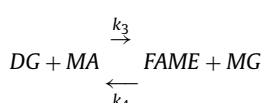
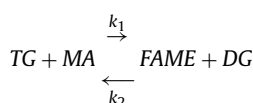
$$\% x = \frac{\text{weight of produced glycerol in grams}}{5} * 100\% \quad (2)$$

2.3. Theoretical consideration

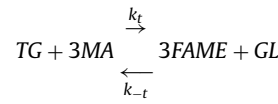
Three kinetic models were suggested, power law kinetics, Eley–Rideal and Langmuir–Hinshelwood mechanisms.

2.3.1. Power law models

First, power law kinetics were tested, both first order and second order reaction models as in the case of using homogeneous catalyst. The mechanism of homogeneous catalyst is illustrated by the following set of reactions.



Overall reaction:



Some assumptions can be taken into consideration in order to simplify studying transesterification reaction kinetics [63,34]. For kinetic studies, some researchers selected the three step reaction to describe transesterification, which is complex and time consuming. This mechanism was replaced by simpler one step kinetics, with respect to triglyceride and methyl ester only, which is the overall transesterification reaction [64]. In the present work the final overall reaction was suggested to be the only one to be used to determine the kinetics [65–68] as the concentration of partial glycerides were negligible compared to methanol, glycerol and oil as well as biodiesel which indicate that these intermediate reactions are fast. The reliability of this assumption was tested statistically with different tests such as R^2 (determination coefficient), t -test and Fisher criterion. The reaction rate may be considered as in Eq. (3).

$$r = k_t * [TG] * [MA]^3 - k_{-t} * [FAME]^3 * [GL] \quad (3)$$

As the concentration of methyl alcohol almost does not change due to its use in large excess so the general rate equation will be:

$$r = K * [TG] - k_{-t} * [FAME]^3 * [GL] \quad (4)$$

where

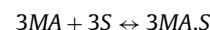
$$r = - \frac{d[TG]}{dt} \quad (5)$$

The rate equation was tested in different forms depending on different assumptions. The following is a brief of the suggested forms and the assumptions led to those forms:

- 1) $r = K * [TG]$ First order in triglyceride concentration without the term of backward reaction. This assumption was suggested due to the high excess of methanol which shifts the reaction in the forward direction.
- 2) $r = K * [TG]^2$ Second order in triglyceride concentration without the term of backward reaction. This assumption was also suggested due to the high excess of methanol which shifts the reaction in the forward direction.
- 3) $r = K * [TG] - k_{-t} * [FAME]^3 * [GL]$ First order in triglyceride concentration and the term of backward reaction was considered.
- 4) $r = K * [TG]^2 - k_{-t} * [FAME]^3 * [GL]$ Second order in triglyceride concentration and the term of backward reaction was considered.

2.3.2. Eley–Rideal kinetics

The suggested mechanism for Eley–Rideal method is illustrated in the following three equilibrium reactions:



The first reaction represents the adsorption of methanol on the active site of catalyst surface. The second step is the surface reaction step which is the determining step. Finally, the third step is desorption of glycerol from the active site of catalyst surface.

Rate equation of Eley–Rideal model

$$r_{Ad} = k_{ad} * C_{MA}^3 * C_V^3 - k_{ad-} * C_{MA,S}^3 \quad (6)$$

$$r_S = k_s * C_{MA,S}^3 * C_{TG} - k_{s-} * C_{FAME}^3 * C_{GL,S} * C_V^2 \quad (7)$$

$$r_D = k_d * C_{GL,S} - k_{d-} * C_{GL} * C_V \quad (8)$$

From (Eq. (6)) the equation of adsorption rate (Eq. (9)) can be obtained:

$$C_{MA,S}^3 = K_{ad}^* * C_{MA}^3 * C_V^3 \quad (9)$$

Assuming that the forward reaction is so fast and its constant has large value. Where:

$$K_{ad}^* = \frac{k_{ad}}{k_{ad-}} \quad (10)$$

If the same procedure is used with desorption step:

$$C_{GL,S} = \frac{1}{K_d} * C_{GL} * C_V \quad (11)$$

$$K_d^* = \frac{k_d}{k_{d-}} \quad (12)$$

Applying site balance

$$C_t = C_V + C_{MA,S} + C_{GL,S} \quad (13)$$

$$C_V = \frac{C_t}{1 + \sqrt[3]{K_{ad}^*} C_{MA} + \frac{1}{K_d^*} C_{GL}} \quad (14)$$

Substituting in (Eq. (7)) the equation of rate of surface reaction, the final form will be:

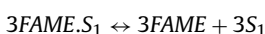
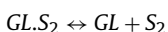
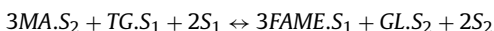
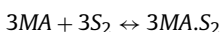
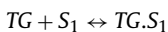
$$r_S = \frac{K' * C_{TG} * C_{MA}^3 - K'' * C_{FAME}^3 * C_{GL}}{\left(1 + \sqrt[3]{K_{ad}^*} C_{MA} + \frac{1}{K_d^*} C_{GL}\right)^3} \quad (15)$$

$$K' = K_{ad}^* * k_s * C_t^3 \quad (16)$$

$$K'' = k_{s-} * C_t^3 \quad (17)$$

2.3.3. Langmuir–Hinshelwood model

In this case there are two assumptions; all species are adsorbed on the active sites of catalyst surface and there are two different types of catalytic active sites. The suggested mechanism for this method is illustrated in the following five equilibrium reactions:



The first two reactions represent the adsorption of soybean oil and methanol on the active sites of catalyst surface. The third step is the surface reaction step which is the determining step. Finally, the last two steps are desorption of glycerol and FAME from the active sites of catalyst surface.

In this case the adsorption and desorption steps will be two for each type. Also site balance calculations will be in two different

Table 3
Chemical Composition of used CCKD.

Concentration by wt%	Main Constituents
7.01	SiO ₂
0.27	TiO ₂
1.90	Al ₂ O ₃
0.05	MnO
2.31	Fe ₂ O ₃ ^{tot.}
1.14	MgO
45.89	CaO
2.49	Na ₂ O
5.60	K ₂ O
0.06	P ₂ O ₅
2.43	SO ₃
6.61	Cl
23.71	LOI

equations as there are two different types of catalytic active sites. The final form of the rate equation for this model will be:

$$r_S = \frac{K_1'' * C_{TG} * C_{MA}^3 - K_2'' * C_{FAME}^3 * C_{GL}}{\left(1 + K_3'' C_{TG} + K_4'' C_{FAME}\right)^3 * \left(1 + K_5'' C_{MA} + K_6'' C_{GL}\right)^3} \quad (18)$$

Least squares method, Runge–Kutta methods for ordinary differential equations and Levenberg–Marquardt algorithm for minimizing objective function (summation of squared error between predicted and observed data) with the aid of “*datafit*” software for curve fitting and data plotting were used to obtain the parameters of each suggested model in each phase. Calculation of determination coefficient (R^2) and minimum of squared error summation method were used to determine the model that best fits the experimental data.

3. Results and discussions

3.1. Catalyst characterization

Table 3 illustrates a typical composition of CCKD used obtained from XRF. It indicates that the calcium oxide content is about 46% as well as total alkalis (Na₂O and K₂O) of about 8% that may contribute in catalyzing transesterification reaction [69,70]. Sieve analysis showed that 56% of particles were retained on the 75 µm sieve and 34% on 63 µm sieve. The percentage of particles crossed 50 µm sieve was too small and negligible. **Figs. 1 and 2** display the morphology and elemental analysis, obtained from EDAX unit, of used CCKD while **Fig. 3** shows the XRD analysis of this CCKD.

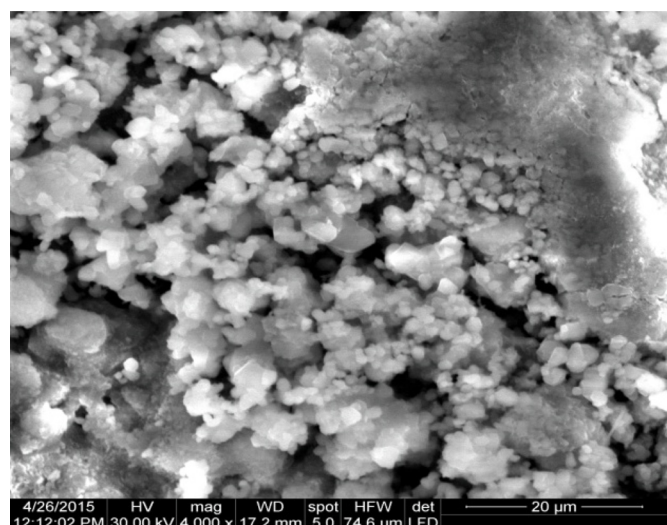


Fig. 1. A typical image of used CCKD by SEM (4000×).

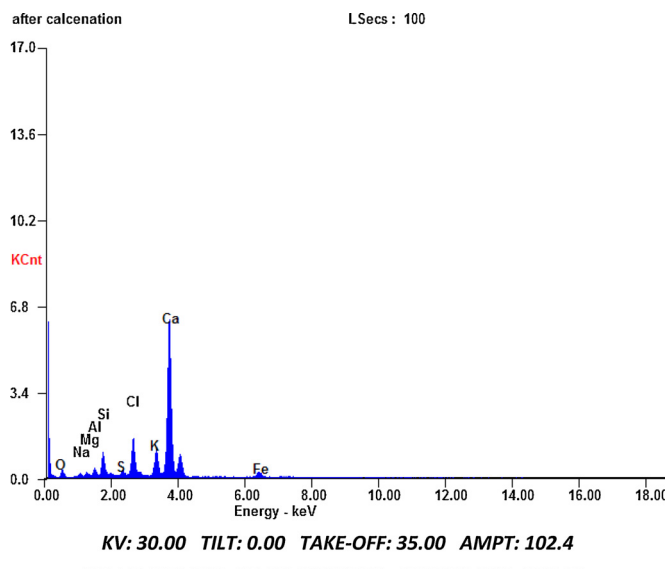


Fig. 2. Elemental Analysis of used CCKD obtained from EDAX unit.

XRD pattern showed five sharp diffraction peaks produced by well-crystallized cubic calcium oxide and some weak and smaller peaks of other components such as $\text{Ca}(\text{OH})_2$ and sodium calcium silicate. **Table 4** summarizes some important physical properties of used CCKD while **Figs. 4** and **5** display the full adsorption-desorption isotherm and multipoint BET plot, respectively. It may be observed that the pore volume and specific surface area are relatively low which indicates that CCKD used is not porous and the transesterification reaction takes place only on the outer surface of the catalyst particles. It was found that the value of (H_-) lies between 15 and 18.4. It was also observed that a solution of CCKD (0.5 g in 20 ml methanol) has a pH of about 12.5 which reveals strong basicity of

Table 4
Physical Properties of used CCKD.

Property	Value unit
Specific Surface Area	17.81 m^2/g
Average Pore Size	13 Å
Pore Volume	0.0115 cc/g
Particle Density	2400 kg/m^3
Bulk Density	700 kg/m^3

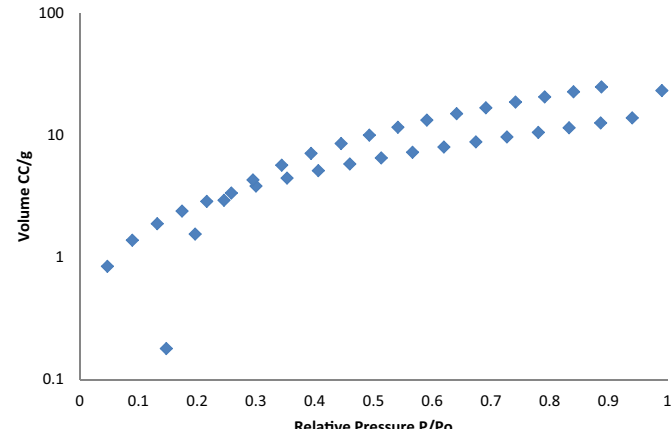


Fig. 4. Adsorption-Desorption Isotherm of used CCKD.

CCKD. Thermal gravimetric analysis of used CKD is illustrated in **Fig. 6**; it may be observed from the figure that, decomposition of calcium hydroxide occurred in the range 350–400 °C [71] while calcium carbonate was decomposed at temperature range from 550 °C to 700 °C [72]. Volatilization of alkali salts could be the cause of the additional weight losses.

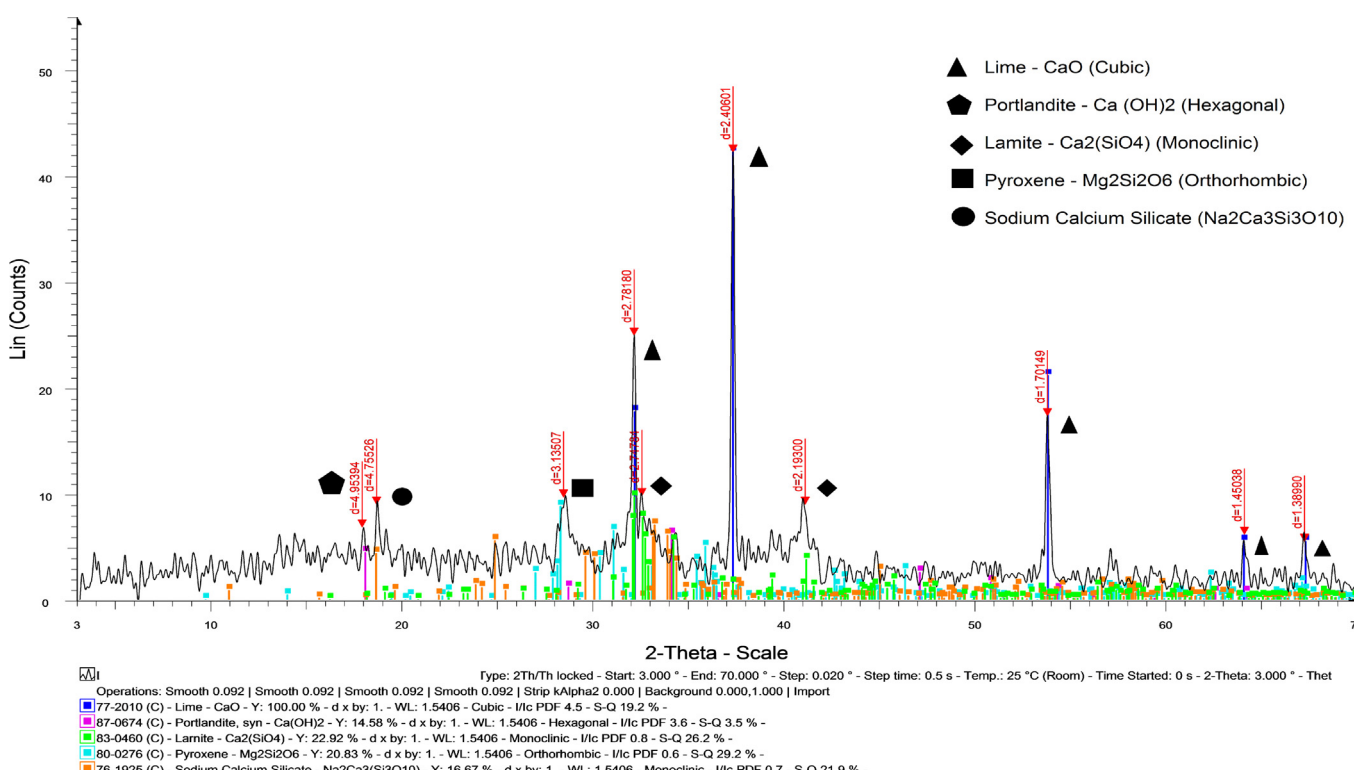


Fig. 3. XRD Pattern of used CCKD.

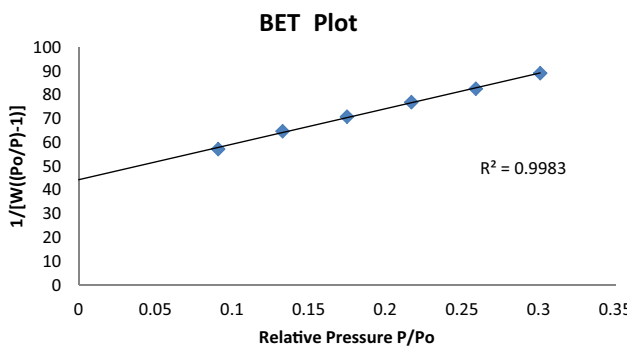


Fig. 5. Multipoint BET Plot.

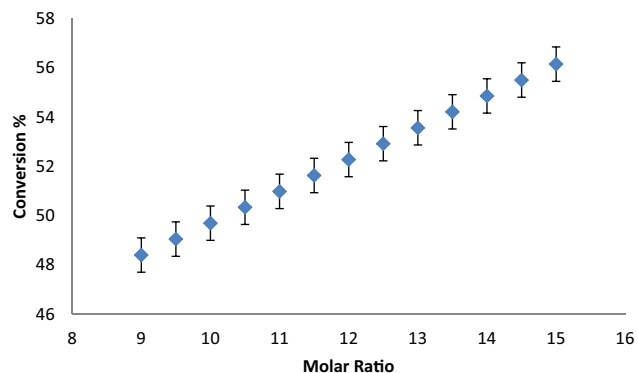


Fig. 8. Effect of molar ratio on conversion (at 3.5% catalyst loading and 3 h reaction time).

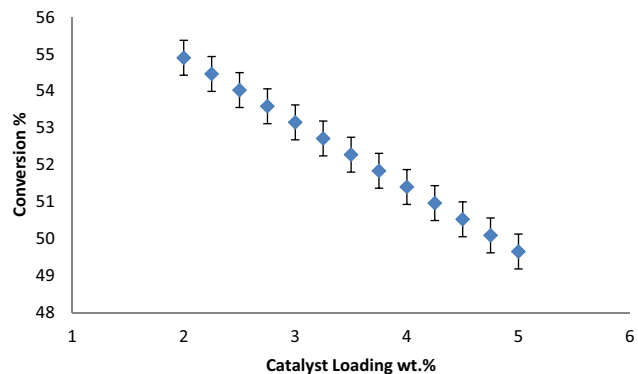


Fig. 9. Effect of catalyst loading on conversion (at 12:1 molar ratio and 3 h reaction time).

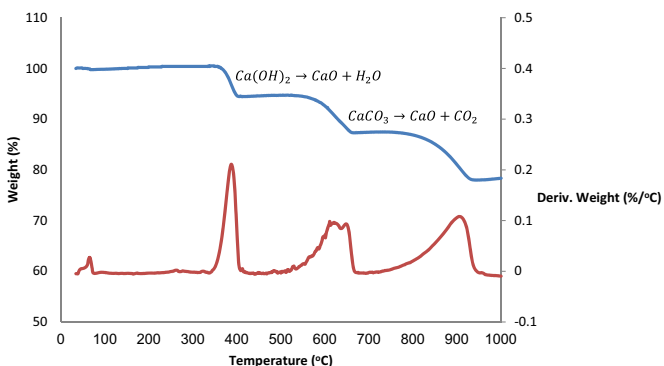


Fig. 6. TGA Pattern of used CKD.

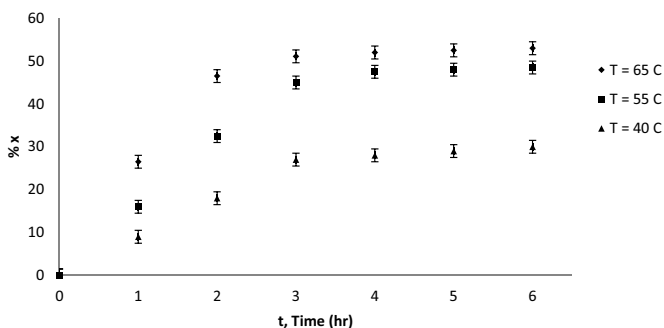


Fig. 7. Effect of temperature on Soybean oil transesterification with methanol using CKD as a catalyst (12:1 molar ratio and 3.5% catalyst loading).

3.2. Experimental results

Transesterification was done using soybean oil and methanol with constant molar ratio of 12:1 and CKD catalyst loading of 3.5% at three different temperatures 40, 55 and 65 °C. The conversions are plotted versus time in Fig. 7.

The effect of molar ratio and catalyst loading on reaction extent were investigated in order to get the optimum of each in soybean oil transesterification using calcined CKD as a heterogeneous catalyst [73]. Figs. 8 and 9 illustrate the effect of these two variables on soybean oil conversion to biodiesel.

The agitation speed was kept at a constant value of 800 rpm; from Fig. 8, it is obvious that using higher excess of methanol (higher methanol to oil ratio) shifts the reaction to the forward path which increases reaction extent as well as its rate. On the other hand, as catalyst loading increases, reaction conversion decreases, that is illustrated in Fig. 9, due to the increase of mass transfer resistance which decreases mass transfer rate and consequently the reaction rate.

The values of reaction parameters, molar ratio of 12:1 and catalyst loading of 3.5%, were chosen for this study for economical reasons and in order to use the generated rate equation in the modeling of an industrial scale reactor for biodiesel production [74]. In this study it was desired to use methanol as low as it could be in order to decrease the cost of reactants to make the process more economic, while in the case of CKD, it was desired to utilize as much as possible of this waste, which produced in huge amounts, as it is relatively cheap (relative to other catalysts such as homogeneous KOH catalyst) which can also increase biodiesel production process feasibility and economy.

3.3. Homogeneous models

These models are suggested due to presence of soluble alkaline oxides (i.e. Na₂O and K₂O) which may contribute in catalyzing transesterification homogeneously as well as leaching of solid oxides. After fitting the experimental data obtained at 65 °C to the first suggested two kinetic models Eqs. (19) and (20) reaction rate ($\text{mol L}^{-1} \text{h}^{-1}$) equations were obtained.

$$r = 0.1637 * C_{TG} \quad (19)$$

$$r = 0.3646 * C_{TG}^2 \quad (20)$$

It was observed that the assumption of second order is better than first order but both of them cannot represent the kinetics of transesterification reaction using calcined CKD as a solid catalyst. Fig. 10 illustrates this interpretation. Scattered points in this figure represent the experimental data while the dashed line is the first order kinetics and the smooth line is the second order kinetics. It is obvious that these two models cannot fit heterogeneously catalyzed transesterification as the error ranges from about 16% to about 35%

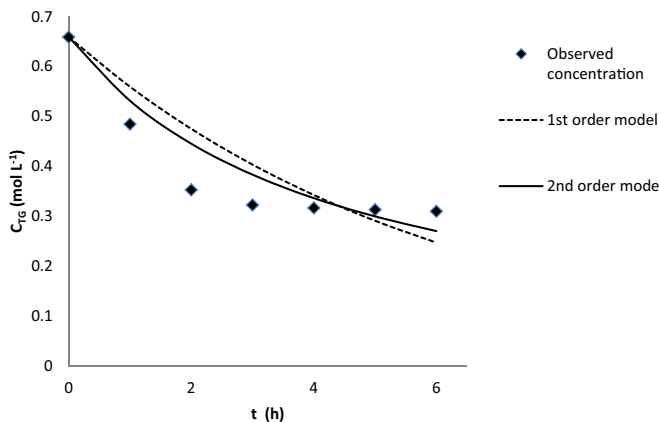


Fig. 10. Irreversible Homogeneous Models.

in the case of first order model, and ranges from 10% to 26% in the case of second order model.

The second phase of generating rate equation was to add the backward reaction term of this reversible reaction. Three models were suggested in this case. The first one was first order with respect to oil concentration and the second one was second order with respect to oil concentration. In both two models methanol concentration was constant. Eq. (21) represents the first order model and Eq. (22) represents second order kinetics at 65 °C.

$$r_s = 0.324 * C_{TG} - 0.2565 * C_{GL} * C_{FAME}^3 \quad (21)$$

$$r_s = 0.5974 * C_{TG}^2 - 0.132 * C_{GL} * C_{FAME}^3 \quad (22)$$

The third suggested model in this phase is to consider a variable methanol concentration. Eq. (23) is the mathematical representation of this model

$$r_s = 0.001 * C_{TG} * C_{MEOH}^3 - 0.1708 * C_{GL} * C_{FAME}^3 \quad (23)$$

These three models showed good results and fitting to the experimental data as the values of determination coefficient for each one of them are 0.9809, 0.9768 and 0.9621, respectively; they will be further discussed and compared to the heterogeneous models in Section 3.5 in order to select the best model that fits the obtained experimental data.

3.4. Heterogeneous catalysis models

For heterogeneous catalytic reactions, kinetics of reaction can be modeled using Eley–Rideal and Langmuir–Hinshelwood models and the results will be illustrated in the following subsections.

3.4.1. Eley–Rideal kinetics model

In this case, two models were suggested. The first one was to consider an irreversible reaction due to high agitation rate and excess methanol. In second model, reaction was considered to be reversible and the term of backward reaction was added. Eqs. (24) and (25) represent the rate equations of these two models at 65 °C.

$$r_s = \frac{0.8043 * C_{TG} * C_{MA}^3}{(1 + 1.0376C_{MA} + 14.7693C_{GL})^3} \quad (24)$$

$$r_s = \frac{0.6731 * C_{TG} * C_{MA}^3 - 139.3176 * C_{FAME}^3 * C_{GL}}{(1 + 1.1876C_{MA} - 2.6739C_{GL})^3} \quad (25)$$

3.4.2. Langmuir–Hinshelwood model

The last generated model is the L-H kinetic model. Triglyceride and FAME are suggested to be adsorbed on the same kind of sites

Table 5
Determination Coefficient (R^2) for Suggested Kinetic Models.

Kinetic Model	R^2
Reversible First order model	0.9809
Reversible Second order model	0.9768
Homogeneous model (variable methanol concentration)	0.9621
Irreversible Eley–Rideal model	0.6339
Reversible Eley–Rideal model	0.9908
Langmuir–Hinshelwood model	0.9628

Table 6
Summation of squared errors for some suggested kinetic models.

Kinetic Model	Summation of squared errors
Reversible First order model	0.00055
Reversible Second order model	0.00204
Homogeneous model (variable methanol concentration)	0.00152
Reversible Eley–Rideal model	0.00027
Langmuir–Hinshelwood model	0.00054

Table 7
Results of t-test.

Parameter	0.6731	-139.3176	1.1876	-2.6739
t-value	158.2763805	32759.89521	279.2587	628.7553
p-value	<0.0001	<0.0001	<0.0001	<0.0001

which are not same kind of sites on which methanol and glycerol are adsorbed. Rate equation of this model at 65 °C is Eq. (26).

$$r_s = \frac{1.2887 * C_{TG} * C_{MA}^3 - 263.4203 * C_{FAME}^3 * C_{GL}}{(1 + 0.9089C_{TG} + 0.2587C_{FAME})^3 * (1 + 0.9085C_{MA} - 2.3998C_{GL})^3} \quad (26)$$

The validity of each rate equation was evaluated by calculating determination coefficient (R^2) for each one. The results of this test are tabulated in Table 5 from which it may be observed that (R^2) ranges from 0.96 to about 0.99 except the value related to the irreversible Eley–Rideal kinetic model which is about 0.634 and the determination coefficient of reversible Eley–Rideal kinetic model has the highest value among the suggested kinetic models which is 0.9908. But as the values are so close so another method should be used to determine which model is the best one to fit the obtained experimental data.

3.5. Selection of best available model

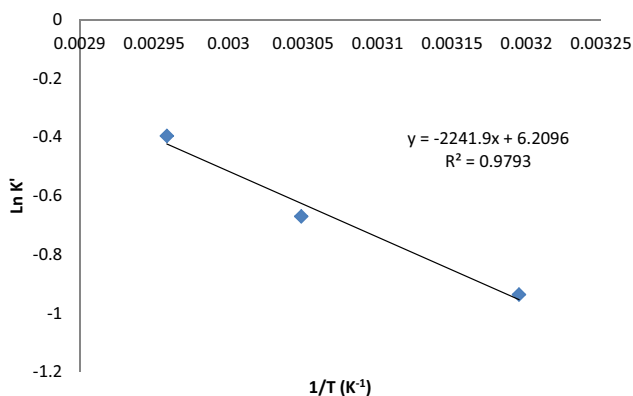
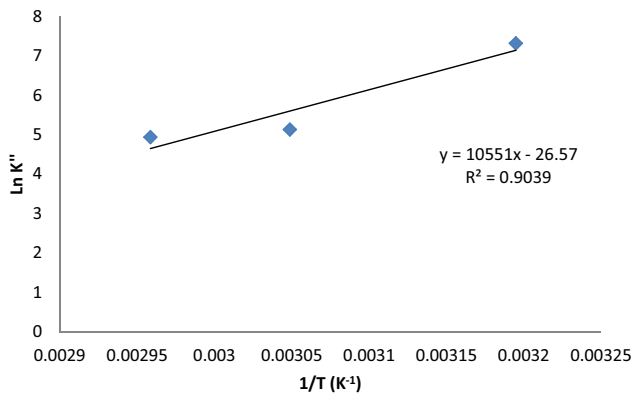
The selection of the most suitable kinetic model that fits the experimental data obtained in the range of present study was done through the least squares method. The concept of this method is to get the summation of squared errors at different points for all models then the best one of them has the least summation of squared errors. Table 6 summarizes the results of applying this method on different models from which it is obvious that models of pure heterogeneous catalyzed reactions have lower summations than those of homogeneous models. The best model that describes the kinetics of Soybean oil transesterification in this study is the reversible Eley–Rideal kinetic model.

The validity of reversible Eley–Rideal model was further tested using Fisher criterion. It was found that $F_{\text{critical}} = 9.5520$ and $F_{\text{calculated}} = 1.8434$ which means that reversible Eley–Rideal model fits the experimental data adequately. On using Chi-square criterion, the critical Chi-square is 11.0705 and the calculated one is 0.0301 which means that the model fairly fits the experimental data. Significance of each parameter was evaluated using t-test at confidence level of 95%. The results of this test are illustrated in Table 7 noting that the critical t-value is 3.1824. Results of this test statistic show that all four parameters are at high significance. The confidence level in these statistical tests was 95%.

Table 8

Constant of Eley–Rideal Rate Equation at Different Temperatures.

Constant	Temperature °C		
	65	55	40
$K' \text{ mol}^{-3} \text{ L}^3 \text{ h}^{-1}$	0.6731	0.5117	0.3921
$K'' \text{ mol}^{-3} \text{ L}^3 \text{ h}^{-1}$	139.3176	168.8005	1508.7005
$K'_{ad} \text{ mol}^{-3} \text{ L}^3$	1.6750	2.4404	3.4901
$K'_d \text{ mol L}^{-1}$	0.3740	0.1312	0.0872

Fig. 11. $\ln K'$ versus $1/T (\text{K}^{-1})$.Fig. 12. $\ln K''$ versus $1/T (\text{K}^{-1})$.

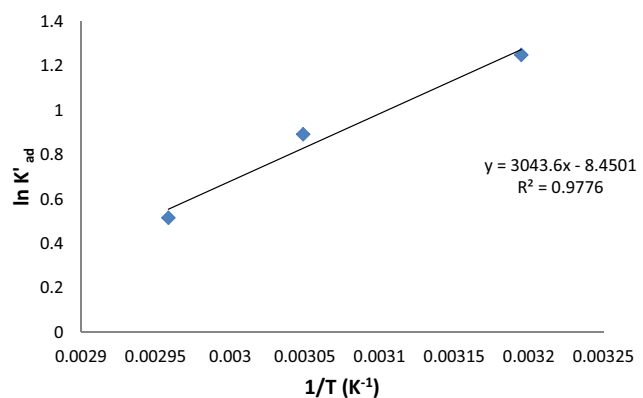
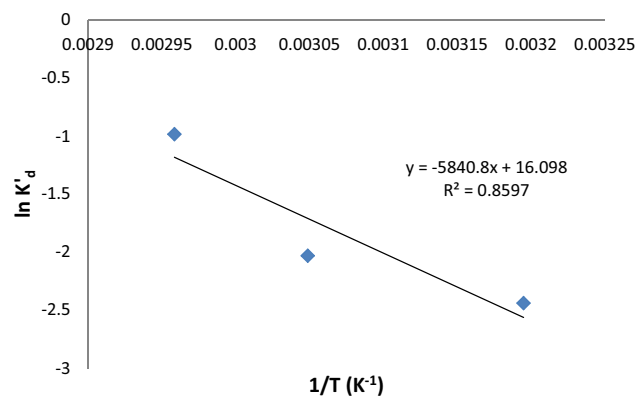
3.6. Activation energies and pre-exponential factors

In order to calculate the activation energies and pre exponential factors of each constant of Eley–Rideal rate equation the experimental data obtained at temperatures 55 °C and 40 °C should be fitted to Eley–Rideal kinetic model. The values of the constants at each temperature are illustrated in Table 8. After obtaining these values, activation energies and pre exponential factors can be calculated graphically by plotting $\ln (k)$ versus $1/T$ where (k) represents each constant and (T) is temperature in Kelvin according to Arrhenius equation. These plots are illustrated in Figs. 11–14 for K' , K'' , K'_{ad} and K'_d , respectively. Table 9 summarizes the results of these calculations.

Table 9

Activation Energies and Pre-exponential Factors.

Constant	Activation Energy KJ/mol	Pre-exponential factor
$K' \text{ mol}^{-3} \text{ L}^3 \text{ h}^{-1}$	18.64	$4.9750 \times 10^{-2} \text{ mol}^{-3} \text{ L}^3 \text{ h}^{-1}$
$K'' \text{ mol}^{-3} \text{ L}^3 \text{ h}^{-1}$	-87.721 (reverse reaction)	$2.8893 \times 10^{-12} \text{ mol}^{-3} \text{ L}^3 \text{ h}^{-1}$
$K'_{ad} \text{ mol}^{-3} \text{ L}^3$	-25.3045	$2.14 \times 10^{-4} \text{ mol}^{-3} \text{ L}^3$
$K'_d \text{ mol L}^{-1}$	48.5621	$9.8 \times 10^{-6} \text{ mol L}^{-1}$

Fig. 13. $\ln K'_{ad}$ versus $1/T (\text{K}^{-1})$.Fig. 14. $\ln K'_d$ versus $1/T (\text{K}^{-1})$.

It should be noticed that the obtained activation energies are the apparent ones, as the reactions followed are not elementary (i.e. overall reactions of a certain mechanism). Even in the case of activation energies of K'_{ad} and K'_d they are equilibrium constants of reversible steps (i.e. adsorption and desorption steps) their activation energies are the difference between the activation energy of forward reaction and of the backward reaction. Now if the activation energy of the forward reaction is higher than the one of backward reaction then the value of the resultant apparent activation energy will be positive while if the activation energy of the forward reaction is lower than the one of backward reaction then the value of the resultant apparent activation energy will be negative.

3.7. Kinetic results using selected model

As the Eley–Rideal model and the reaction taking place in a batch reactor the gradient of concentration with respect to time (at 65 °C) could be represented mathematically by Eq. (27).

$$-\frac{dC_{TG}}{dt} = \frac{0.6731 * C_{TG} * C_{MA}^3 - 139.3176 * C_{FAME}^3 * C_{GL}}{(1 + 1.1876C_{MA} - 2.6739C_{GL})^3} \quad (27)$$

Since the concentration of any species is a function of conversion and the initial concentration of limiting reactant; the gradient of conversion with respect to time will be a function of conversion only as shown in Eq. (28).

$$C_{TG_0} * \frac{dx}{dt} = \frac{-705.1491x^4 - 41.6287x^3 + 180.343x^2 - 318.4046x + 176.2672}{-163.6043x^3 + 1327.6086x^2 - 3591.0721x + 3237.8503} \quad (28)$$

where $C_{TG_0} = 0.6588 \text{ mole L}^{-1}$

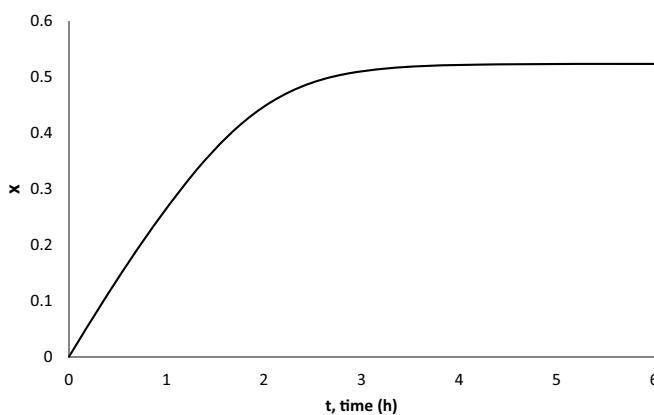


Fig. 15. Conversion versus Time.

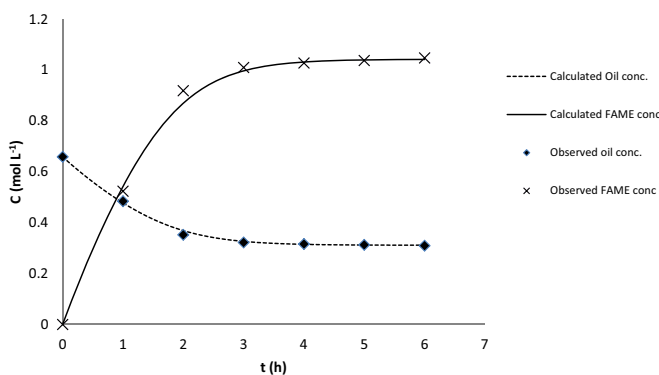


Fig. 16. Concentration of oil and biodiesel versus Time.

Solving this differential equation using Polymath, Fig. 15 was obtained in which a maximum conversion of 52.36% was reached after 6 h with an error of about 1.21% where the experimentally observed conversion at this time was about 53% consequently the concentration of any species could be plotted versus time. Fig. 16 represents the concentration of oil and produced biodiesel along reaction time.

3.8. Study of mass transfer resistances

In this section different mass transfer resistances were examined to show that the reaction is only kinetically controlled and that the conditions applied as well as catalyst (calcined CKD) properties eliminated mass transfer resistances.

3.8.1. External mass transfer resistance

Table 10 shows the physical properties of the reaction mixture along reaction time at 65 °C.

Diffusivities presented in the previous table were calculated using Wilke-Chang equation. At the first stages of the reaction, diffusivity of oil into the mixture equals about $(6 \times 10^{-10}) \text{ m}^2/\text{s}$ diffusivity of oil in methanol as the concentrations of biodiesel and glycerol are low enough to be neglected. As the reaction proceeds

Table 10
Average Physical Properties of Reaction Mixture.

Property	Value
Viscosity (cP)	8
Density (kg/m³)	800
Diffusivity (oil in methanol) (m^2/s)	6×10^{-10}
Diffusivity (oil in biodiesel) (m^2/s)	3×10^{-11}
Diffusivity (oil in glycerol) (m^2/s)	3×10^{-13}

the diffusivity of oil inside the mixture decreases due to the increase of biodiesel and glycerol concentrations. In the present case the diffusivity of oil in the mixture after the proposed reaction time (six hours) equals about 1.55×10^{-10} as the conversion is about 53% and this means that biodiesel has a significant contribution on oil diffusivity inside the mixture. Glycerol concentration along reaction time is low enough to be neglected as the conversion is relatively low besides using methanol in high excess.

After determination of oil diffusivity inside the mixture mass transfer coefficient can be calculated using Frossling correlation illustrated in Eq. (29).

$$Sh = 2 + 0.6 * Re^{1/2} * Sc^{1/3} \quad (29)$$

Before using the correlation, Reynolds and Schmidt numbers should be calculated. Eqs. (30) and (31) present the form of Reynolds and Schmidt numbers.

$$Re = \frac{\rho * d_p * U}{\mu} \quad (30)$$

$$Sc = \frac{\mu}{\rho * D_{AB}} \quad (31)$$

where, $U = \omega * D$; U is linear velocity in m/s, ω is angular velocity in rps and D is reactor diameter in m. Reaction took place using a constant agitation speed of 800 RPM and the reactor diameter was about 0.1 m, so the linear velocity of the catalyst particle is about 4.2 m/s. Maximum catalyst particle size is about 82.5 μm (the worst case). Using these calculations as well as physical properties mentioned in Table 1 values of Reynolds and Schmidt numbers can be obtained. These values are 34,56 and 31,746 for Reynolds and Schmidt numbers respectively. Substituting in Frossling correlation, Sherwood number is obtained at a value of about 113.68 then mass transfer coefficient can be calculated from Eq. (32). The resultant value of mass transfer coefficient is about 1.563 m/h .

$$Sh = \frac{k_m * d_p}{D_{AB}} \quad (32)$$

To insure that the kinetic study is intrinsic and no external mass transfer limitations take place during reaction, concentration of oil at catalyst surface should be equal to or to be with a value near the concentration of oil in solution bulk. One way to estimate the concentration of oil at catalyst surface is to assume that the rate of reaction equals rate of mass transfer, then surface concentration can be obtained, Eq. (33) represents the mathematical formula of this statement.

$$r = k_m * (C_{Ab} - C_{As}) \quad (33)$$

Table 11 summarizes the results of estimated surface concentrations and the diffusivity of oil in reaction mixture along reaction time.

It can be noticed that oil diffusivity decreases with time and this is due to generation of biodiesel and glycerol. Also it may be observed that the values of concentrations of oil at catalyst surface are near to the values of oil concentrations in the bulk of reaction mixture which means that the external mass transfer resistance is negligible and that verifies the first hypothesis that the reaction is not controlled by external diffusion. To make sure that the reaction is completely controlled by surface reaction and there is no contribution of mass transfer resistances in controlling the reaction, internal mass transfer should be evaluated.

3.8.2. Internal mass transfer resistance

The internal mass transfer will be investigated by three approaches and proved to be negligible and the reaction takes place only on the surface of catalyst particle.

The average pore diameter of calcined CKD particle used is about 13 Å while MacLeod [34] reported that the molecular diameter of

Table 11

Estimated Surface Concentrations and Oil Diffusivities along Reaction Time.

Time (h)	Oil Bulk Concentration (mol L^{-1})	Oil Surface Concentration (mol L^{-1})	Oil Diffusivity into the mixture (m^2/s)
0.5	0.571529412	0.459801	3.20928E-10
1.5	0.418352941	0.33403	1.97076E-10
2.5	0.337317647	0.317923	1.63663E-10
3.5	0.3192	0.307205	1.57685E-10
4.5	0.314588235	0.311211	1.56233E-10
5.5	0.311294118	0.307902	1.55212E-10

triglyceride is about 16 \AA , this means that triglyceride molecule cannot enter inside the catalyst particle and that the reaction takes place only on catalyst surface.

It was investigated that there is a relation between catalyst particle size and effectiveness factor. MacLeod [34] stated that the effectiveness factor for transesterification reaction reaches unity for particle sizes up to 1 mm when oil diffusivity takes the value of $5 \times 10^{-10} \text{ m}^2/\text{s}$, i.e. oil diffusing in methanol, while on considering the oil diffuses in biodiesel, i.e. value of the diffusivity is about $3 \times 10^{-11} \text{ m}^2/\text{s}$, effectiveness factor reaches unity for particle sizes up to $100 \mu\text{m}$. Comparing these investigations with the present case, maximum particle size of $82.5 \mu\text{m}$ and minimum diffusivity of $1.55 \times 10^{-10} \text{ m}^2/\text{s}$, it may be observed that the effectiveness factor equals unity which indicates that the internal mass transfer resistance is negligible.

The third approach to prove that the internal mass transfer resistance is to calculate Thiele modulus then calculating effectiveness factor. If the effectiveness factor equals unity then the internal mass transfer resistance is negligible. It is noticed that the reaction can follow irreversible first order kinetic model with a small error in the first stages. This observation can simplify calculations of Thiele modulus and leads to make it take the form presented in Eq. (34).

$$\varphi = \frac{V_p}{S_p} * \sqrt{\frac{k_{rxn}}{D_{eff}}} \quad (34)$$

where, $D_{eff} = D_{AB} \times \varepsilon/\tau$ where D_{eff} is oil effective diffusivity, D_{AB} is oil diffusivity, ε is catalyst porosity and τ is catalyst tortuosity. The range of tortuosity in most catalysts is from 1 to $\sqrt{3}$ but it can reach higher values such as 3 or 4 [75]. In the case of porosity, it ranges from 0.1 to 0.9 in most known porous catalysts. Calculating the effective diffusivity using the worst cases reported in literature for porosity and tortuosity values (i.e. lowest value of porosity and highest value of tortuosity) 0.1 and 4 respectively and substituting in Eq. (34) with this value gives a Thiele modulus of about 0.046 (very low value). Relation between Thiele modulus and effectiveness factor, after substitution with the proposed reaction rate formula in the differential equation that relates Thiele modulus and effectiveness factor and integration of the resultant equation, is shown in Eq. (35) which is used to calculate effectiveness factor which is found to have the value of about 0.9998, almost 1, that indicates a negligible internal mass transfer resistance.

$$\eta = \frac{3}{\varphi^2} * (\varphi * \coth \varphi - 1) \quad (35)$$

4. Conclusion

From the above investigations it may be concluded that the kinetics of transesterification of soybean oil with methanol using calcined CKD as a heterogeneous catalyst may be represented using Eley–Rideal model based on three-step mechanism where the surface reaction step is the controlling one. This result was detected after many theoretical and statistical analyses using experimental and well known models and applying F-test criterion. This was also approved for all parameters with a p -value < 0.0001 for all of them. The calculated activation energies of Eley–Rideal model constants K' , K'' , K'_{ad} and K''_{ad} are 18.6400, -87.7210 , -25.3045 and

48.5621 KJ/mol (apparent activation energies of reversible reactions). After examination of different mass transfer limitations (internally and externally), it was demonstrated that the reaction is independent from diffusion limitations as the external and internal mass transfer resistances were found to be negligible.

Acknowledgements

The authors would like to thank Prof. Said S.E.H. Elnashaie and Prof. Magdi F. Abadir very much for their support.

Appendix A. Supplementary data

Supplementary data associated with this article can be found, in the online version, at <http://dx.doi.org/10.1016/j.apcatb.2017.01.008>.

References

- [1] N. Sh. El-Gendy, S.F. Deriase, Waste eggshells for production of biodiesel from different types of waste cooking oil as waste recycling and a renewable energy process, *Energy Sources Part A* 37 (2015) 1114–1124.
- [2] A. Datta, B.K. Mandal, Use of jatropha biodiesel as a future sustainable fuel, *Energy Technol. Policy* 1 (2014) 8–14.
- [3] S.R. Medipally, F.M. Yusoff, S. Banerjee, M. Shariff, Microalgae as sustainable renewable energy feedstock for biofuel production, *BioMed Res. Int.* 2015 (2015) 13 (Article ID 5195).
- [4] P. Verma, M.P. Sharma, G. Dwivedi, Impact of alcohol on biodiesel production and properties, *Renew. Sustain. Energy Rev.* 56 (2016) 319–333.
- [5] P. Verma, M.P. Sharma, Review of process parameters for biodiesel production from different feedstocks, *Renew. Sustain. Energy Rev.* 62 (2016) 1063–1071.
- [6] A.S. Silitonga, H.H. Masjuki, H. Chyuan Ong, T. Yusaf, F. Kusumo, T.M.I. Mahlia, Synthesis and optimization of Hevea brasiliensis and Ricinus communis as feedstock for biodiesel production: a comparative study, *Ind. Crops Prod.* 85 (2016) 274–286.
- [7] P. Verma, G. Dwivedi, M.P. Sharma, Comprehensive analysis on potential factors of ethanol in Karanja biodiesel production and its kinetic studies, *Fuel* 188 (2017) 586–594.
- [8] G. Dwivedi, M.P. Sharma, Application of Box–Behnken design in optimization of biodiesel yield from Pongamia oil and its stability analysis, *Fuel* 145 (2015) 256–262.
- [9] A.K. Azad, M.G. Rasul, M.M.K. Khan, S.C. Sharma, M.A. Hazrat, Prospect of biofuels as an alternative transport fuel in Australia, *Renew. Sustain. Energy Rev.* 43 (2015) 331–351.
- [10] J. Kosinkova, A. Doshi, J. Maire, Z. Ristovski, R. Brown, T.J. Rainey, Measuring the regional availability of biomass for biofuels and the potential for microalgae, *Renew. Sustain. Energy Rev.* 49 (2015) 1271–1285.
- [11] P. Verma, M.P. Sharma, Comparative analysis of effect of methanol and ethanol on Karanja biodiesel production and its optimization, *Fuel* 180 (2016) 164–174.
- [12] P. Verma, M.P. Sharma, G. Dwivedi, Prospects of bio-based alcohols for Karanja biodiesel production: an optimization study by response surface methodology, *Fuel* 183 (2016) 185–194.
- [13] K. Mu’azu, I.A. Mohammed-Dabo, S.M. Waziri, A.S. Ahmed, I.M. Bugaje, U.A.S. Zanna, Kinetic modeling of transesterification of Jatropha curcas seed oil using heterogeneous catalyst, *Eng. Technol.* 2 (2015) 87–94.
- [14] E. Aransiola, M. Daramola, T. Ojumu, B. Solomon, S. Layokun, Homogeneously catalyzed transesterification of nigerian Jatropha curcas oil into biodiesel: a kinetic study, *Mod. Res. Catal.* 2 (2013) 83–89.
- [15] A.-Birla, B. Singh, S.N. Upadhyay, Y.C. Sharma, Kinetics studies of synthesis of biodiesel from waste frying oil using a heterogeneous catalyst derived from snail shell, *Bioresour. Technol.* 106 (2012) 95–100.
- [16] Thomas J. Davison, Chinedu Okoli, Karen Wilson, Adam F. Lee, Adam Harvey, Julia Woodford, Jhuma Sadhukhan, Multi-scale modeling of heterogeneously catalyzed transesterification reaction process: an overview, *RSC Adv.* 3 (2013) 6226–6240.
- [17] D. Krishnan, A kinetic study of biodiesel in waste cooking oil, *Afr. J. Biotechnol.* 11 (2012) 9797–9804.

[18] J.F. Portha, F. Allain, V. Coupard, A. Dandeu, E. Girot, E. Schaeer, L. Falk, Simulation and kinetic study of transesterification of triolein to biodiesel using modular reactors, *Chem. Eng. J.* 207–208 (1 (October)) (2012) 285–298, <http://dx.doi.org/10.1016/j.cej.2012.06.106>.

[19] F. Allain, J.F. Portha, E. Girot, L. Falk, A. Dandeu, V. Coupard, Estimation of kinetic parameters and diffusion coefficients for the transesterification of triolein with methanol on a solid $ZnAl_2O_4$ catalyst, *Chem. Eng. J.* 283 (2016) 833–845.

[20] K. Ankur, W. Karen, F.L. Adam, S. Jhuma, Kinetic modeling studies of heterogeneously catalyzed biodiesel synthesis reactions, *Ind. Eng. Chem. Res.* 50 (2011) 4818–4830.

[21] R. Klaewkla, M. Arend, W.F. Hoelderich, in: H. Nakajima (Ed.), A Review of Mass Transfer Controlling the Reaction Rate in Heterogeneous Catalytic Systems, *Mass Transfer – Advanced Aspects*, InTech, Rijeka, Croatia, 2011, ISBN: 978-953-307-636-2. available from: <http://www.intechopen.com/books/mass-transfer-advanced-aspects/a-review-of-mass-transfer-controlling-the-reaction-rate-in-heterogeneous-catalytic-systems>.

[22] H.S. Fogler, *Elements of Chemical Reaction Engineering*, 3rd edition, Prentice-Hall, New Delhi, India, 2005.

[23] M.E. Davis, R.J. Davis, *Fundamentals of Chemical Reaction Engineering*, 1st edition, McGraw Hill, New York, USA, 2003.

[24] H. Noureddini, D. Zhu, Kinetics of transesterification of soybean oil, *J. Am. Oil Chem. Soc.* 74 (1997) 1457–1463.

[25] M.E. Bambase, N. Nakamura, J. Tanaka, M. Matsumura, Kinetics of hydroxide-catalyzed methanolysis of crude sunflower oil for the production of fuel-grade methyl esters, *J. Chem. Technol. Biotechnol.* 82 (2007) 273–280.

[26] S.K. Karmee, D. Chandna, R. Ravi, A. Chadha, Kinetics of base-catalyzed transesterification of triglycerides from Pongamia oil, *J. Am. Oil Chem. Soc.* 83 (2006) 873–877.

[27] G. Vicente, M. Martínez, J. Aracil, A. Esteban, Kinetics of sunflower oil methanolysis, *Ind. Eng. Chem. Res.* 44 (2005) 5447–5454.

[28] D. Darnoko, M. Cheryan, Kinetics of palm oil transesterification in a batch reactor, *J. Am. Oil Chem. Soc.* 77 (2000) 1263–1267.

[29] V.C. Eze, The Use of Meso-Scale Oscillatory Baffled Reactors for Rapid Screening of Heterogeneously Catalyzed Biodiesel Production Reactions, PhD Thesis, School of Chemical Engineering and Advanced Materials, Newcastle University, United Kingdom, 2014.

[30] T.F. Dossin, M.F. Reyniers, G.B. Marin, Kinetics of heterogeneously MgO -catalyzed transesterification, *Appl. Catal. B: Environ.* 62 (2006) 35–45.

[31] H. Hattori, M. Shima, H. Kabashima, Alcoholysis of ester and epoxide catalyzed by solid bases, *Stud. Surf. Sci. Catal.* 130 (2000) 3507–3512.

[32] Y. Xiao, L. Gao, G. Xiao, J. Lv, Kinetics of the transesterification reaction catalyzed by solid base in a fixed-bed reactor, *Energy Fuels* 24 (2010) 5829–5833.

[33] M. Di Serio, R. Tesser, L. Pengmei, E. Santacesaria, Heterogeneous catalysts for biodiesel production, *Energy Fuels* 22 (2008) 207–217.

[34] C. Macleod, Evaluation of Heterogeneous Catalysts for Biodiesel Production, PhD Thesis, School of Chemical Engineering and Advanced Materials, Newcastle University, United Kingdom, 2008.

[35] A.P. Singh Chouhan, A.K. Sarma, Modern heterogeneous catalysts for biodiesel production: a comprehensive review, *Renew. Sustain. Energy Rev.* 15 (2011) 4378–4399.

[36] G.E.G. Muciño, R. Romero, A. Ramírez, M.J. Ramos, R.B. Jiménez, R. Natividad, Kinetics of transesterification of sunflower oil to obtain biodiesel using heterogeneous catalysis, *Int. J. Chem. Reactor Eng.* 14 (2016) 929–938.

[37] D. Kumar, A. Ali, Transesterification of low-quality triglycerides over a Zn/CaO heterogeneous catalyst: kinetics and reusability studies, *Energy Fuels* 27 (2013) 3758–3768.

[38] M. Feyzi, G. Khajavia, Kinetics study of biodiesel synthesis from sunflower oil using $Ba/Sr/ZSM-5$ nano-catalyst, *Iran. J. Catal.* 6 (2016) 29–35.

[39] A. Nambo, C.M. Miralda, J.B. Jasinski, M.A. Carreon, Methanolysis of olive oil for biodiesel synthesis over ZnO nanorods, *React. Kinet. Mech. Catal.* 114 (2015) 583–595.

[40] G. Moradi, M. Mohadesi, Z. Hojabri, Biodiesel production by CaO/SiO_2 catalyst synthesized by the sol-gel process, *Reac. Kinet. Mech. Cat.* 113 (2014) 169–186.

[41] N. Kaur, A. Ali, Biodiesel production via ethanalysis of jatropha oil using molybdenum impregnated calcium oxide as solid catalyst, *RSC Adv.* 5 (2015) 13285–13295.

[42] M. Kaur, A. Ali, An efficient and reusable Li/NiO heterogeneous catalyst for ethanalysis of waste cottonseed oil, *Eur. J. Lipid Sci. Technol.* 117 (2015) 550–560.

[43] N. Kaur, A. Ali, Preparation and application of $Ce/ZrO_2-TiO_2/SO_4^{2-}$ as solid catalyst for the esterification of fatty acids, *Renew. Energy* 81 (2015) 421–431.

[44] N. Kaur, A. Ali, Lithium zirconate as solid catalyst for simultaneous esterification and transesterification of low quality triglycerides, *Appl. Catal. A: Gen.* 489 (2015) 193–202.

[45] M.R. Avhad, M. Sánchez, E. Peña, A. Bouaid, M. Martínez, J. Aracil, J.M. Marchetti, Renewable production of value-added jojobyl alcohols and biodiesel using a naturally-derived heterogeneous green catalyst, *Fuel* 179 (2016) 332–338.

[46] G.R. Moradi, M. Mohadesi, M. Ghanbari, M.J. Moradi, Sh. Hosseini, Y. Davoodbeygi, Kinetic comparison of two basic heterogeneous catalysts obtained from sustainable resources for transesterification of waste cooking oil, *Biofuel Res. J.* 6 (2015) 236–241.

[47] M.R. Avhad, M. Sánchez, E. Peña, A. Bouaid, M. Martínez, J. Aracil, J.M. Marchetti, Modeling chemical kinetics of avocado oil ethanalysis catalyzed by solid glycerol-enriched calcium oxide, *Energy Convers. Manage.* 126 (15 (October)) (2016) 1168–1177, <http://dx.doi.org/10.1016/j.enconman.2016.07.060>.

[48] M. Gaonkar, A.P. Chakraborty, Application of eggshell as fertilizer and calcium supplement tablet, *Int. J. Innov. Res. Sci. Eng. Technol.* 5 (2016) 3520–3525.

[49] A.M. King'ori, A review of the uses of poultry eggshells and shell membranes, *Int. J. Poult. Sci.* 10 (2011) 908–912.

[50] C. McLaughlin, P. Rose, D.C. Aldridge, Making the best of a pest: the potential for using invasive zebra mussel (*Dreissena polymorpha*) biomass as a supplement to commercial chicken feed, *Environ. Manage.* 54 (2014) 1102–1109.

[51] A.M. Khan, N. Fatima, M.S. Hussain, K. Yasmeen, Biodiesel production from green seaweed *Ulva fasciata* catalyzed by novel waste catalysts from Pakistan steel industry, *Chin. J. Chem. Eng.* 24 (8 (August)) (2016) 1080–1086, <http://dx.doi.org/10.1016/j.cjche.2016.01.009>.

[52] J.X. Wang, K.T. Chen, B.Z. Wen, Y.H.B. Liao, C.C. Chen, Transesterification of soybean oil to biodiesel using cement as a solid base catalyst, *J. Taiwan Inst. Chem. Eng.* 43 (2012) 215–219.

[53] B.K. Uprey, W. Chaiwong, C. Ewelike, S.K. Rakshit, Biodiesel production using heterogeneous catalysts including wood ash and the importance of enhancing byproduct glycerol purity, *Energy Convers. Manage.* 115 (2016) 191–199.

[54] H.H.M. Darweesh, Utilization of cement kiln by-pass dust waste as a source of CaO in ceramic industry, *Silic. Ind.* 66 (2001) 47–52.

[55] M.H. El-Awady, T.M. Sami, Removal of heavy metals by cement kiln dust, *Bull. Environ. Contam. Toxicol.* 59 (1997) 603–610.

[56] M.K. Rahman, S. Rehman, O.S.B. Al-Amoudi, Literature review on cement kiln dust usage in soil and waste stabilization and experimental investigation, *IJRAS* 7 (2011) 77–87.

[57] M.S. Konsta-Gdoutos, S.P. Shah, Hydration and properties of novel blended cements based on cement kiln dust and blast furnace slag, *Cem. Concr. Res.* 33 (2003) 1269–1276.

[58] A. Sreekrishnavilasam, M.C. Santagata, Development of Criteria for the Utilization of Cement Kiln Dust (CKD) in Highway Infrastructures. FHWA/IN/JTRP-2005/10, Final Report for Joint Transportation Research Program, School of Civil Engineering, Purdue University, Indiana, 2006.

[59] O.E. Agwu, A.N. Okon, F.D. Udo, A comparative study of diesel oil and soybean oil as oil-based drilling mud, *J. Pet. Eng.* 2015 (2015) 10, Article ID 828451.

[60] F. Shahidi, Bailey's industrial oil and fat products Six Volume Set, Vol. 2, sixth edition, John Wiley & Sons, Inc., 2005, pp. 584–586 (Ch. 13).

[61] N. Asikin-Mijana, H.V. Lee, Y.H. Taufiq-Yap, Synthesis and catalytic activity of hydration-dehydration treated clamshell derived CaO for biodiesel production, *Chem. Eng. Res. Des.* 102 (2015) 368–377.

[62] Z.A. Shaharatun Nur, Y.H. Taufiq-Yap, M.F. Rabiah Nizah, S.H. Teo, O.N. Syazwani, A. Islam, Production of biodiesel from palm oil using modified Malaysian natural dolomites, *Energy Convers. Manage.* 78 (2014) 738–744.

[63] H.I. El Shimi, N.K. Attia, S.T. El Sheltawy, G.I. El Diwani, Reactive extraction processing of spirulina-platensis microalgae to produce biodiesel: kinetics study, *Int. J. Eng. Sci. Innov. Technol.* 4 (2015) 338–349.

[64] P. Verma, M.P. Sharma, Review of process parameters for biodiesel production from different feedstocks, *Renew. Sustain. Energy Rev.* 62 (2016) 1063–1071.

[65] N.B. Talib, S. Triwahyono, A.A. Jalil, C.R. Mamat, N. Salamun, N.A.A. Fatah, S.M. Sidik, L.P. Teh, Utilization of a cost effective Lapindo mud catalyst derived from eruption waste for transesterification of waste oils, *Energy Convers. Manage.* 108 (2016) 411–421.

[66] G. Moradi, M. Mohadesi, S. Hosseini, Y. Davoodbeygi, R. Moradi, DM water plant sedimentation as a cheap and waste source of catalyst for biodiesel production, *Int. J. Chem. Reactor Eng.* 14 (2015) 113–124.

[67] I. Lukić, Ž. Kesić, S. Maksimović, M. Zdujić, J. Krstić, D. Skala, Kinetics of heterogeneous methanolysis of sunflower oil with $CaO-ZnO$ catalyst: influence of different hydrodynamic conditions, *Chem. Ind. Chem. Eng. Q.* 20 (2014) 425–439.

[68] D.J. Vučić, D. Comić, A. Zarubica, R. Micic, G. Boskovi, Kinetics of biodiesel synthesis from sunflower oil over CaO heterogeneous catalyst, *Fuel* 89 (2010) 2054–2061.

[69] S.L. Martínez, R. Romero, R. Natividad, J. González, Optimization of biodiesel production from sunflower oil by transesterification using Na_2O/NaX and methanol, *Catal. Today* 220–222 (2014) 12–20.

[70] R. Peña, R. Romero, S.L. Martínez, R. Natividad, A. Ramírez, Characterization of KNO_3/NaX catalyst for sunflower oil transesterification, *Fuel* 110 (2013) 63–69.

[71] R.Sh. Mikhail, S. Brunauer, L.E. Copeland, Kinetics of the thermal decomposition of calcium hydroxide, *J. Colloid Interface Sci.* 21 (1996) 394–404.

[72] T.R. Rao, Kinetics of calcium carbonate decomposition, *Chem. Eng. Technol.* 19 (1996) 373–377.

[73] E.G. Al-Sakkari, S.T. El-Sheltawy, M.F. Abadir, N.K. Attia, G. El-Diwani, Investigation of cement kiln dust utilization for catalyzing biodiesel production via response surface methodology, *Int. J. Energy Res.* (2016) 3635 (in press) <http://onlinelibrary.wiley.com/doi/10.1002/er.3635/epdf>.

[74] S.T. El-Sheltawy, E.G. Al-Sakkari, M. Fouad, Modeling and process simulation of biodiesel production from soybean oil using cement kiln dust as a heterogeneous catalyst, *J. Solid Waste Technol. Manag.* 42 (2016) 313–324.

[75] T.O. Salmi, J.P. Mikkola, J.P. Warna, *Chemical Reaction Engineering and Reactor Technology*, CRC Press/Taylor and Francis, 2011, pp. 550.